



# An adaptive reduction scheme to model reactive flow

Ipsita Banerjee, Marianthi G. Ierapetritou \*

*Department of Chemical and Biochemical Engineering, Rutgers University, Piscataway, NJ 08854, USA*

Received 10 August 2004; received in revised form 1 June 2005; accepted 5 July 2005

Available online 16 November 2005

## Abstract

Detailed simulation of reactive flow systems using complex kinetic mechanisms consisting of hundreds of species is a computationally demanding task. In practice, to alleviate the computational complexity, the reactive flow models use a skeletal kinetic model instead of the detailed mechanism. However, the reduced chemistry models can accurately predict the detailed model only over a limited range of conditions. Since the reactive flow simulation encounters a broad range of conditions, using a single reduced model throughout the simulation incorporates inaccuracy into the predictive capacity of the flow model. In this paper, an adaptive scheme is presented, which aims at developing different reduced models to address the changing conditions of the flow simulation, thereby maintaining high accuracy throughout the simulation with relatively simple chemistry models. A new approach is developed for the analysis of the range of validity of the reduced model, which is highly nonconvex, for which the conventional techniques do not perform well. Finally, a procedure to implement the adaptive chemistry in different flow simulations is presented.

© 2005 The Combustion Institute. Published by Elsevier Inc. All rights reserved.

*Keywords:* Adaptive chemistry; Kinetic model reduction; Combustion; Mathematical modeling; Optimization

## 1. Introduction

Over the past couple of decades detailed kinetic networks have been developed to model combustion processes. Although kinetic simulation comprising hundred of species and thousand of reactions is not a constraint in homogeneous systems, detailed simulation of complex reacting flow systems having strong coupling of heat and mass transfer is still computationally prohibitive. The stiffness of the embedded kinetics often makes the integration of chemical source terms the most expensive step. In practice, to allevi-

ate the computational complexity, the reacting flow models use a skeletal kinetic model instead of the detailed mechanism. There has been considerable effort toward reduced representation of detailed kinetic mechanisms to alleviate the computational workload, a detailed review of which can be obtained in Tomlin et al. [1]. Most of the techniques are based on the concept of timescale separation.

The first such technique is the quasi-steady state approximation (QSSA) [2], which involves setting certain species in steady state and certain reactions in partial equilibrium. QSSA is a relatively simple technique to apply, although it involves considerable *chemist's intuition* to know which species to set in steady state and which reactions in partial equilibrium. Tools have been developed to aid this process [3], but they still require a set of appropriate model

\* Corresponding author.

*E-mail address:* [marianth@sol.rutgers.edu](mailto:marianth@sol.rutgers.edu)  
(M.G. Ierapetritou).

problems in which to examine the rates. Hence the method has still not been fully automated, and is essentially a hand-powered analytical technique. Chen [4] developed an interactive computer assisted reduction mechanism code (CARM) for the automatic generation of reduced models, based on the QSS assumption. It has been used in different problems and found to have a broad range of applicability [5,6].

Frenklach [7] suggested the *solution mapping* approach, where the model responses are expressed as simple algebraic functions (usually polynomials) in terms of the model variables. These algebraic functions, called *response surfaces*, are obtained by carrying out several thousand computer simulations using the complete kinetic model. If the fitted function has fewer variables than that of the original mechanism, a reduced-dimension model is produced.

A more recent effort toward automation of mechanism reduction has resulted in the intrinsic low-dimensional manifold (ILDM) and computational singular perturbation (CSP) [8] methods. They offer considerable advantages over QSSA but are significantly more complicated to implement. The ILDM method [9] explicitly computes the low-dimensional manifolds on which the slow chemistry evolves in the reaction state space, and then tabulates the computed results in a lookup table for later use in reactive flow code. The CSP method uses a transformation of the system basis vectors to automatically compute the optimum steady state and partial equilibrium relationship. Unlike ILDM, it gives rise to an explicit reduced mechanism, thus providing better understanding of the rate-limiting chemistry.

An alternative to mechanism reduction is the in situ adaptive tabulation (ISAT) technique proposed by Pope [10]. The basic idea behind ISAT is to integrate the chemical source term and store the reaction mapping and sensitivity information in a binary tree data structure for later use. For subsequent calculations, for points within a small distance of the previously tabulated points, direct integration is avoided by estimating the reaction mapping using multilinear interpolation. Any reaction mapping that cannot be interpolated with sufficient accuracy is generated by direct integration and stored in a table.

Another suggested approach toward automation of the mechanism reduction is the mathematical programming-based approach [11–13], the basic idea of which is followed in the present work. This approach is based on determining the reactions that can be excluded from the detailed mechanism while still retaining desired accuracy in the prediction of the profiles of certain important species. This approach renders great flexibility in the generation of the reduced model, which can overcome the shortcomings of the previous methods. Following this approach it is

possible to generate reduced models with specific user defined property and accuracy, which gives the flexibility to generate different reduced models to serve different purposes. Also it gives an estimate of the error due to the use of the reduced model.

For most of the existing reduction schemes mentioned before, the simplified kinetic model represents the chemical activity tolerably well in a limited region of the flow field and is not accurate over the entire temperature/composition space of interest. In the absence of detailed study of the range of validity of reduced model, the CFD simulation uses the same reduced model over the entire range of conditions, thereby incorporating significant error in the simulation. Moreover, in many burner simulations there are large areas of relatively little or no chemical activity and small regions of intense chemical reaction. Schwer et al. [14] presented a burner simulation using three reduced sets of nonreactive chemistry models and a single reduced reactive chemistry model, along with the detailed methane combustion model. Accurate prediction of the flow simulation was obtained by using the nonreactive models for considerable regions of the simulation. Hence, when a single chemistry model is used for such simulation, the reaction equations are unnecessarily integrated even in the nonreactive zones [14]. To overcome these problems an adaptive chemistry approach has been proposed in this work where different chemical behavior of the reactive flow simulations is represented by different reduced models, thereby maintaining sufficient accuracy with significantly reduced models. Though this work concentrates only on combustion systems, the proposed method is general and can be applied to any reacting system.

The paper is organized as follows, Section 2 presents a methodology for generation of the reduced mechanism, followed by a feasibility analysis of the reduced mechanism presented in Section 3. Section 4 is a detailed development of the adaptive chemistry scheme and Section 5 deals with the integration of the proposed adaptive scheme with the flow simulation. A summary of the overall approach and detailed discussion of the areas requiring further attention are presented in Section 6.

## 2. Mechanism reduction

Over the past couple of decades there has been considerable effort toward development of suitable technique for reduction of complex kinetic mechanism to enable detailed simulation of reactive flow models. The main challenge of this effort is in the development of a completely automated procedure for the generation of reduced models, which maintains the required accuracy and can be easily incorporated

in the CFD codes. The mathematical programming based approach was found to meet these requirements, and has the additional advantage of generating reduced models tailored to desired mechanism characteristics. A detailed description of the formulation of mechanism reduction problem and the solution technique is presented in this section.

2.1. Formulation of mechanism reduction

The reduction technique adopted in this work follows the main idea of the mathematical programming approach proposed by Androulakis [11]. This approach assumes that the detailed kinetic network is known with considerable accuracy, and it aims at eliminating species and reactions that are of lower importance in determining the profiles of the desired species. Hence the objective is to retain the minimum number of species and reactions in the reduced model, while the constraint is to predict the profiles of the important species with desired accuracy. For a typical combustion system, the number of reactions far exceeds the total number of species. For example, methane combustion following the GRI-3.0 mechanism involves 53 species and 325 reactions [15]. Since the dimension of the problem directly relates to the number of involved variables, which is the number of species for species reduction and number of reactions for reaction reduction, the efficiency of the solution procedure can be increased by first starting with a lower number of variables. Hence the first step is the reduction of total number species of the system, the formulation of which as an optimization problem for an isobaric batch reactor is given by

$$\min_{\lambda \in \Lambda^{N_s}} \sum_{k=1}^{N_s} \lambda_k \tag{1}$$

subject to  $\chi \leq \delta$ ,

$$\chi = \left( \sum_{k \in \kappa} \int_{t_I}^{t_F} \left( \frac{y_k^{\text{reduced}}(t) - y_k^{\text{full}}(t)}{y_k^{\text{full}}(t)} \right)^2 dt + \int_{t_I}^{t_F} \left( \frac{T_k^{\text{reduced}}(t) - T_k^{\text{full}}(t)}{T_k^{\text{full}}(t)} \right)^2 dt \right)^{1/2}, \tag{2}$$

$$\frac{dy_k(t)}{dt} = \frac{R_k M_k}{\rho}, \quad k = 1, \dots, N_s, \tag{3}$$

$$\frac{dT}{dt} = - \sum_{k=1}^{N_s} \frac{R_k M_k h_k}{\rho \bar{C}_p}, \tag{4}$$

$$R_k = \sum_{i=1}^{N_r} \left( \prod_{s=1}^{N_s} (\lambda_k)_i \right) (v_{k_i}^r - v_{k_i}^f) q_i, \tag{5}$$

$$q_i = \mathcal{K}_{f_i} \prod_{k=1}^{N_s} X_k^{v_{k_i}^f} - \mathcal{K}_{r_i} \prod_{k=1}^{N_s} X_k^{v_{k_i}^r}, \tag{6}$$

$$\mathcal{K}_{f_i} = K_{f_i} T^{b_i} e^{-E_{f_i}/RT},$$

$$\mathcal{K}_{r_i} = K_{r_i} T^{b_i} e^{-E_{r_i}/RT}, \tag{7}$$

$$\langle \lambda_k \rangle_i = \begin{cases} \lambda_k & \text{if species } k \text{ participates in reaction } i, \\ 0 & \text{otherwise,} \end{cases}$$

where  $\lambda_k$  is a binary variable used to denote the presence ( $\lambda_k = 1$ ) or absence ( $\lambda_k = 0$ ) of a particular species. The objective function  $\sum_{k=1}^{N_s} \lambda_k$  represents the total number of species in the reduced set, which has to be minimized, subject to a specified accuracy ( $\delta$ ). The integral error measure  $\chi$ , given by Eq. (2), defines the approximation error of the trajectories of the key observable quantities for the interval of interest. In the above formulation,  $y_k$  denotes the mass fraction, whereas  $X_k$  represents the molar concentration of species  $k$  used in the calculation of the reaction rates. Equations (3) and (4) represent the material and energy balances for the reactor model, where  $R_k$  is the net rate of production of species  $k$ ;  $M_k$  is the molecular weight of species  $k$ ;  $\rho$  denotes the mixture density, which is a function of composition and temperature.  $R_k$  is evaluated from the knowledge of intrinsic rates  $q_i$  of individual reactions and stoichiometry, as given by Eq. (5). For combustion systems,  $q_i$  is described by the power law expression of mass-action kinetics, as given by Eq. (6). The temperature dependence of the specific reaction rate constant is given by the Arrhenius law (Eq. (7)).

Solution of the above problem will give rise to a reduced model having a smaller number of species than the detailed model. In the process of species reduction, the number of reactions is also indirectly reduced. When a particular species is taken out of the system by assigning the corresponding  $\lambda_s$  to 0, all the reactions in which that species participates are also removed from the system. Hence the resulting model will consist of a reduced number of species and reactions as compared to the original model. Further reduction can be achieved based on the fact that not all the reactions in which the important species participates are equally important. Hence a second step of reaction reduction is performed over the intermediate reduced model. The formulation of reaction reduction is given by

$$\min_{\lambda \in \Lambda^{N'_R}} \sum_{i=1}^{N'_R} \lambda_i$$

subject to  $\chi \leq \delta$ ,

where

$$\chi = \left( \sum_{k \in \kappa} \int_{t_I}^{t_F} \left( \frac{y_k^{\text{reduced}}(t) - y_k^{\text{full}}(t)}{y_k^{\text{full}}(t)} \right)^2 dt + \int_{t_I}^{t_F} \left( \frac{T_k^{\text{reduced}}(t) - T_k^{\text{full}}(t)}{T_k^{\text{full}}(t)} \right)^2 dt \right)^{1/2},$$

$$\frac{dy_k(t)}{dt} = \frac{R_k M_k}{\rho}, \quad k = 1, \dots, N_s,$$

$$\frac{dT}{dt} = - \sum_{k=1}^{N_s} \frac{R_k M_k h_k}{\rho \bar{C}_p},$$

$$R_k = \sum_{i=1}^{N'_r} \lambda_i (v_{k_i}^r - v_{k_i}^f) q_i, \quad (8)$$

where  $\lambda_i$  is a binary variable corresponding to each reaction present in the species-reduced model ( $N'_r$ ), which determines if a reaction ( $i$ ) is present in the network. If a particular reaction can be neglected, then the corresponding  $\lambda_i = 0$ .

Formulation (1)–(7) of mechanism reduction corresponds to an integer nonlinear programming problem that has been solved using genetic algorithms (GA), following the work of Edwards et al. [16]. GA [17,18] represent a class of search and optimization procedures that are patterned after the biological process of natural selection and they lend themselves to solution of a wide range of optimization problems. When GA are applied to an optimization problem, each optimization variable is typically encoded as a string of bits, and these strings are appended together to form a chromosome. Each individual in a population has a particular chromosome value that can be decoded to evaluate the parameter values and objective function, also called the fitness function. Populations are evolved through several generations until the objective function cannot be improved any further.

In the mathematical model (1)–(7) the optimization variables are the  $N_s$  binary variables associated with the species, while in model (8) the variables are the  $N_r$  binary variables associated with the reactions. Hence parameterization for GA is straightforward since each binary variable  $\lambda$  becomes a bit in the GA chromosome. For a particular combination of  $\lambda$  the reduced differential equation sets are integrated to evaluate the discrepancy function. Since GA cannot explicitly handle nonlinear constraints of an optimization problem, there has been considerable research toward efficient constraint handling while using GA. Most of the constraint handling methods are based on the concept of (exterior) penalty functions [18] that penalize the infeasible solution and try to solve an

unconstrained problem using a modified fitness function. The unconstrained optimization for problem (8) can be formulated as

$$\min_{\lambda \in \Lambda^{N'_r}} \sum_{r=1}^{N'_r} \lambda_r + (\text{penalty} \times \max\{0, \chi - \delta\}), \quad (9)$$

where the penalty term becomes zero when the constraint is not violated ( $\chi < \delta$ ), and it takes the value of a large positive quantity (penalty  $\times (\chi - \delta)$ ) otherwise. Note that the penalty coefficient needs to be large enough to ensure that all the infeasible solutions have a fitness value worse than any of the feasible solutions. Unlike classical search and optimization methods, the GA approach begins its search with a random set of solutions, instead of just one solution.

For the solution of problem (8), the first step of the GA procedure involves the random generation of a large population of binary strings (reaction combinations) where each member of the population represents a reduced reaction set. For each reduced set within the initial population the corresponding ODEs are integrated to evaluate the discrepancy function and hence the fitness function, as given in Eq. (9). The integration is performed using LSODE [19], while the rate expressions and all the necessary thermodynamic properties are evaluated using the CHEMKIN-III package [20]. The generated population of solutions are modified by the GA operators (reproduction, crossover, mutation) to create new and better populations. This procedure is repeated until a predefined termination criterion is satisfied. Following this procedure, mechanism reduction was performed for methane combustion, with the detailed mechanism described by GRI-3.0 consisting of 53 species and 325 reactions [15]. The GA simulation was performed with a population size of 10, which was evolved through 500 generations. The initial conditions under which reduction was performed are  $O_2$  mass fraction of 0.468255,  $CH_4$  mass fraction of 0.290531, and temperature of 1208.64 K. The species reduction with an allowable error of 0.01 resulted in a reduced set consisting of 21 species and 99 reactions. Fig. 1 illustrates the performance of the reduced set in predicting the temperature and  $CH_4$  profiles. The predicted temperature profile has 0.1% deviation from the detailed model, while the  $CH_4$  profile was predicted with 0.5% error. The reaction reduction is then performed over this reduced set with the same allowable error, which resulted in the final reduced set consisting of 17 species and 29 reactions. Fig. 2 illustrates the temperature and  $CH_4$  profiles predicted by this final reduced set. The average CPU time required to obtain the final reduced set is 7000 s.

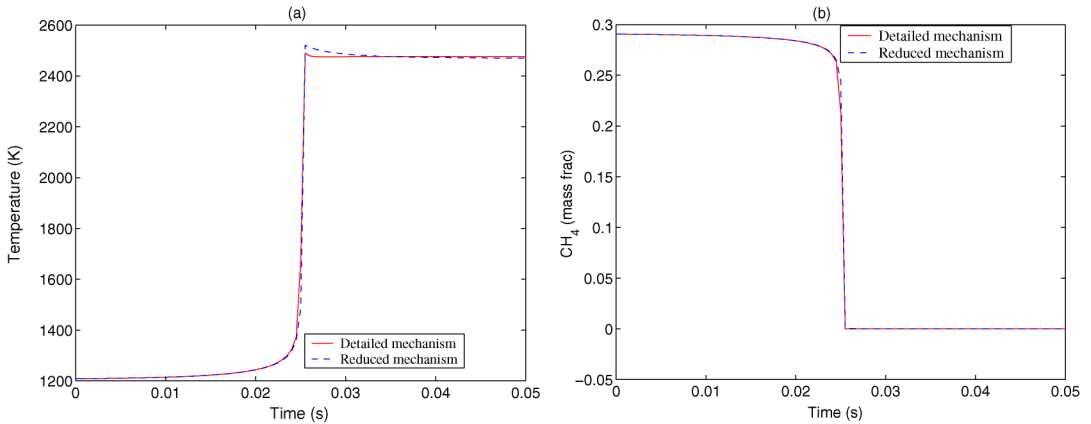


Fig. 1. Performance of species reduction in the prediction of (a) temperature and (b)  $\text{CH}_4$  profiles. The reduced model used consists of 21 species, 99 reactions.

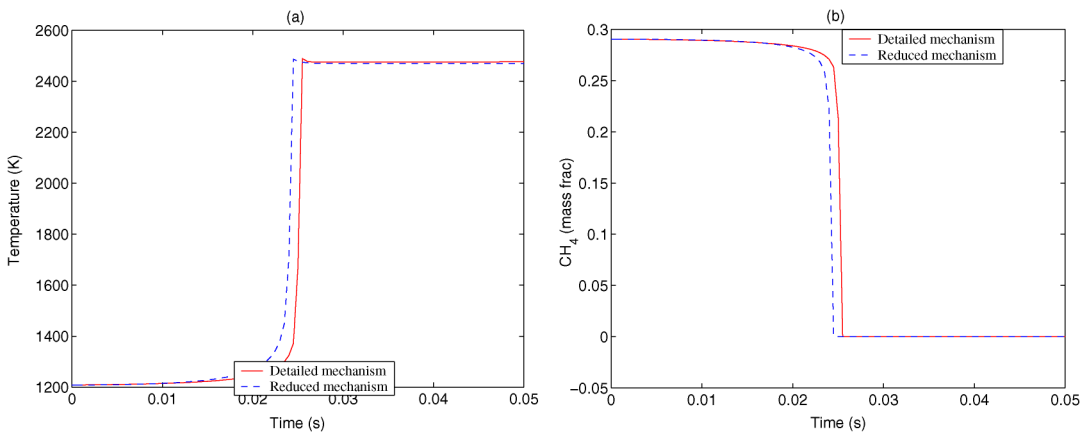


Fig. 2. Performance of reaction reduction in the prediction of (a) temperature and (b)  $\text{CH}_4$  profiles. The reduced model used consists of 17 species, 29 reactions.

## 2.2. Computational savings from mechanism reduction

The computational savings achieved by the reduced kinetic model is due to lower function evaluation and Jacobian evaluation costs. The cost of function evaluation may be expressed as sum of three terms [21],

$$\text{CPU}_{\text{fe}} = \text{CPU}_{\text{re}} + \text{CPU}_{\text{se}} + \text{CPU}_{\text{te}}, \quad (10)$$

where  $\text{CPU}_{\text{fe}}$  is the total CPU cost for a function evaluation of kinetic model,  $\text{CPU}_{\text{re}}$  is the cost of evaluating the reaction rate vector  $q_i$ ,  $\text{CPU}_{\text{se}}$  is the cost of multiplying the stoichiometric matrix ( $\nu$ ) by the reaction rate vector, and  $\text{CPU}_{\text{te}}$  represents all other costs including those for computing various thermodynamic properties. As observed by Bhattacharjee et al. [21],  $\text{CPU}_{\text{se}}$  is a function of the sparsity of the stoichiometric matrix. While elimination of species from

the kinetic model will directly reduce the total number of ODEs to be integrated, elimination of both species and reaction will reduce the nonzero entries of the stoichiometric matrix, as shown in Table 1. However, the density of the matrix (nonzero entries/ $N_s \times N_r$ ) increases with reduction in the size of the mechanism. Table 1 compares the CPU requirement of different reduced models with the detailed GRI-3.0 methane mechanism. It is observed that by reducing the kinetic model to 29 species and 126 reactions from the original size of 53 species and 325 reactions, the CPU requirement can be reduced by almost 84%. For the cases of 22 species, 81 reactions, and 22 species, 35 reactions, the number of ODEs to be integrated remains the same since the same number of species is the same. Even then there is considerable reduction of CPU requirement from 13.87 to 5.57 ms, which is attributed to reaction reduction, which reduces the entries of the stoichiometric matrix.

Table 1  
Computational savings by mechanism reduction

Size of mechanism		Nonzero entries in stoichiometric matrix	Matrix density	CPU <sub><math>v_i q_i</math></sub> (ms)	CPU <sub>cumulative</sub> (ms)
$N_{\text{species}}$	$N_{\text{reaction}}$				
53	325	1227	0.0712	129.21	190.3
29	126	461	0.126	15.87	29.57
22	81	291	0.163	6.07	13.87
22	35	131	0.17	2.11	5.57
20	30	112	0.187	1.3	3.9
20	22	84	0.191	0.54	1.83

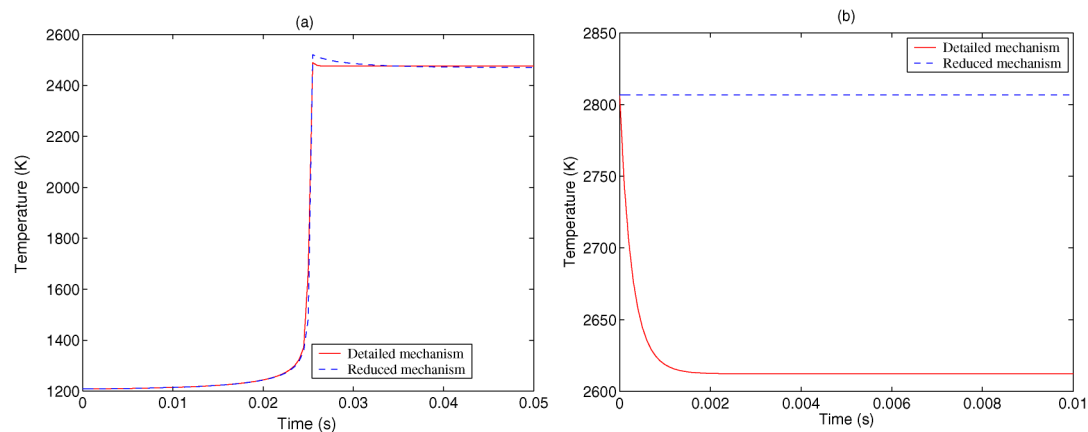


Fig. 3. Performance of the reduced mechanism (a) under nominal conditions of reduction and (b) at conditions away from the nominal.

### 3. Range of validity of reduced mechanisms

A single reduced mechanism has the property of predicting the profiles of the observed species within a certain user-defined accuracy under the initial conditions of species concentration and temperature at which the reduction was performed. If this same mechanism is integrated under vastly different conditions, there is no guarantee of the accuracy of prediction of the reduced model. This is illustrated in Fig. 3, where in plot (a) the integration was performed under the same conditions at which the reduction was performed, namely  $\text{O}_2$  mass fraction = 0.468255,  $\text{CH}_4$  mass fraction = 0.290531 and  $T = 1208.64$  K, whereas in plot (b) the integration was performed under different conditions of  $\text{O}_2$  mass fraction =  $1.28092 \times 10^{-12}$ ,  $\text{CH}_4$  mass fraction =  $1.13365 \times 10^{-4}$ , and  $T = 2806.78$  K. It is observed that although the reduced model predicts the temperature profile under the nominal conditions with great accuracy, under conditions away from the nominal its performance deteriorates significantly.

Hence it is necessary to quantify the range of species concentrations in which the reduced model can predict the species profiles within user-defined accuracy. This leads to the problem of feasibility

analysis, formulated in [22] for process synthesis applications. The idea of feasibility/flexibility analysis was developed in the context of chemical process design and operation, where an important problem is to maintain feasible steady-state operation for a range of uncertain conditions that may be encountered during plant operation. Thus the design flexibility can be defined as the ability of a design to tolerate and adjust to variations in parameter conditions which may be encountered during operation. The feasible region of a reduced model can be similarly defined as the range of species concentration and temperature over which the error constraint is satisfied ( $\chi \leq 0$ ), where  $\chi$  is the measured deviation error evaluated by integration of the detailed and reduced model. The actual validity range of the reduced set is obtained by performing a grid search in the space of temperature,  $\text{O}_2$  concentration and  $\text{CH}_4$  concentration and solving the full and reduced models under different initial conditions and evaluating the error. An examination of this validity range showed that the feasible region is highly non-convex, nonsmooth, and sometimes even disjoint, as shown in Fig. 4. The detailed mechanism used in this simulation is the GRI-3.0 methane combustion mechanism consisting of 53 species and 325 reactions, which was reduced to 17 species and 59 reactions.

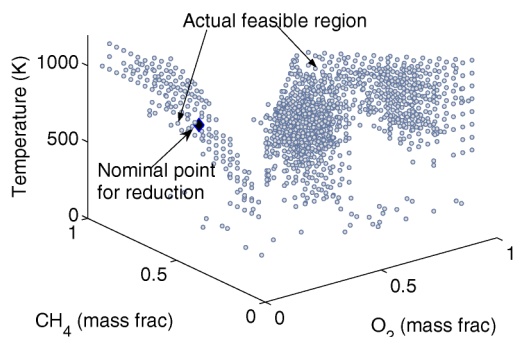


Fig. 4. Feasible region of a reduced model of GRI-3.0 mechanism involving 17 species and 59 reactions.

The conventional techniques for feasibility analysis are largely limited by their assumptions of convexity and continuity of the corresponding model; hence the application of conventional feasibility analysis techniques to estimate such nonconvex regions will lead to erroneous results. A new technique is thus developed for this purpose, based on the idea of surface reconstruction [23]. Surface reconstruction techniques have the capacity for identifying nonconvex, even disjoint surfaces, given a set of points representing an object. To use this technique, first one needs a set of sample points representing the *shape* of the feasible region. However, since the evaluation of the error function is an expensive operation, performing grid search for every reduced set is not feasible. Also, in most of the problems, the feasible region covers only a very restricted region of the entire parameter space. Hence sampling techniques covering the entire range of uncertain parameters prove to be inefficient, particularly when evaluation of the process constraint is an expensive operation. Most of the common sampling techniques sample the parameters space based on the distribution of the uncertain parameter, which is assumed to be uniform for the present system. Under this assumption it will result in uniform sampling of the entire parameter space, irrespective of whether the sampled points are feasible or not. A new sampling technique is thus used here which takes advantage of the fact that typically a small section of the entire parameter space is feasible. The sampling problem is formulated as an optimization problem and is solved using GA. The use of GA as the solution procedure proves to be efficient for this problem since it has the inherent property of concentrating around regions of good solutions, which is the feasible solution for the problem addressed here.

The purpose of the sampling step is to have a good approximation of the feasible space by performing minimum number of evaluation of the expensive feasibility function. The variables in the formulated optimization problem are the initial conditions of species

concentration and temperature, and the objective is to maximize the total number of feasible points in the search space. With this aim, the formulation of the sampling problem as an optimization problem is given by

$$\begin{aligned} & \max \sum \theta_{\text{feas}} \\ & \text{subject to } (\chi)_{\theta_{\text{feas}}} \leq 0, \end{aligned} \quad (11)$$

where  $\theta_{\text{feas}}$  is a set of feasible points representing conditions of species concentration and temperature at which the reduced set is valid. The idea is to maximize the sampled feasible space; hence whenever a chosen value of  $\theta$  satisfies the constraint function, it improves the objective function, but when a condition is not feasible, it is rejected. Solving this problem using GA reduces the required number of function evaluations by minimizing the unnecessary evaluation of the infeasible parameter space. The variables of the formulated optimization problem are continuous; hence to solve  $t$  using GA, the variables are encoded as a string of bits, and these strings are appended together to form a chromosome. The solution procedure starts by generating a large population of solution, which are evolved through several generations by applying different operators. The first operator applied to a population in a genetic algorithms is the reproduction operator. The primary objective of the reproduction operator is to emphasize good solutions and eliminate bad solutions in a population. This is achieved by first identifying above-average solutions in a population, making multiple copies of the good solutions, and eliminating bad solutions from the population in order to accommodate multiple copies of the good solution. Some common methods for achieving this are *tournament selection*, *proportionate selection*, and *ranking selection* [17]. While reproduction can make more copies of the good solution and eliminate bad solution, however, it cannot create a new solution. The crossover operator is applied next to take care of that, where two strings are picked randomly from the mating pool at random and some portions of the strings are swapped among themselves to create two new strings. If the new strings created by a crossover are good, more copies of them will be generated by the reproduction operator in the next mating pool. Otherwise if the new strings are not good, it will not survive beyond next generation, since reproduction will eliminate them.

The working principle of GA is that by application of its three operators, the number of strings with similarities at certain string positions has been increased from initial population to the new population. These similarities, referred to as *schema* in the GA literature, represent a set of strings with similarities at certain string positions. Thus the *schema* can be thought of

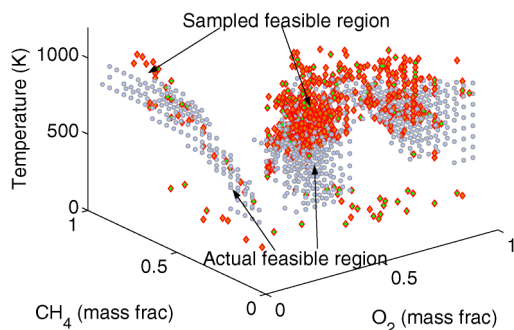


Fig. 5. Sampled feasible region of a reduced model of GRI-3.0 mechanism.

as representing certain regions in the search space, or specific ranges of the parameter value. Hence by having more copies of a schema with a better function value, one can reach the optimal solution without searching the entire variable space, but by manipulating only a few instances of the search space.

This feature of GA is of particular importance for the present problem since only a limited region of the variable space is feasible. Thus exploring the entire variable space to have an idea of the feasible region becomes computationally expensive.

Fig. 5 illustrates the sampled feasible region as compared to the actual feasible region obtained by grid search. An estimate of the points in the composition space at which the reduced mechanism retains its validity having been obtained, the next step is to obtain a mathematical description of this feasible region. This is analogous to the problem of surface reconstruction, where the problem definition is that given a set of points, the shape formed by these points is to be determined. A mathematically rigorous definition of the shape of points was introduced by Edelsbrunner et al., who proposed a generalization of the convex hulls, which are referred to as  $\alpha$  shape. The notion of  $\alpha$  shape has been extensively applied in automatic mesh generation and geometric modeling, molecular structure and protein folding analysis, distribution of point sets, e.g., galaxies in the universe, etc.

The  $\alpha$  shape of a finite point set  $S$  is a polytope that is uniquely determined by  $S$  and a parameter  $\alpha$ . It expresses the intuitive notion of the *shape* of  $S$  and controls the level of detail reflected by the polytope. The original paper on  $\alpha$  shapes [24] defines the concept in two dimensions. An extension to three dimensions, together with an implementation, is reported in [25]. The value of  $\alpha$  controls the level of details of the reconstructed shape. For  $\alpha \rightarrow 0$ , the  $\alpha$  shape of  $S$  degenerates to the point set  $S$ , whereas for  $\alpha \rightarrow \infty$ , reproduces the convex hull of the point set. Mandal and Murthy [26] present a systematic methodology for selecting the value of  $\alpha$  by calculating the mini-

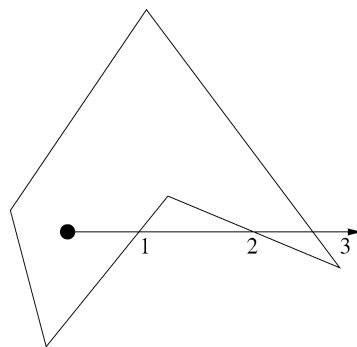


Fig. 6. Point-in-polygon test: odd number of intersections means point is inside, even number of intersections means point is outside.

mum spanning tree of the sampled data points ( $n$ ) and evaluating the sum of edge weights of the MST ( $l_n$ ). The appropriate value of  $\alpha$  is then given by  $\sqrt{l_n/n}$ .

When applied to the problem of feasibility analysis, the aim is to have a mathematical estimate of the range of conditions over which the reduced mechanism is feasible. Hence, the input to  $\alpha$  shape is a set of conditions under which a mechanism is feasible, which has already been identified by the previous procedure. The output from  $\alpha$  shape is points of the original data set, which lies on the boundary of the feasible region. These points can now be joined by a straight line in two dimensions, or by a triangle in three dimensions, to obtain a polygonal representation of the feasible region. Hence, by this procedure, the feasible region is represented by a piece wise linear approximation.

Having identified the boundary points of the feasible region, the next step involves determination of whether a particular point belongs to the feasible region. This can be done by using one of the point-in-polygon tests [27] to determine whether a point is inside a polygon or outside it. One way to determine whether a point is inside a region is the ray-tracing algorithm, which states that a point is inside a polygon if, for any semi-infinite ray from this point, there are an odd number of intersections of the ray with the polygon's edges (Fig. 6). Conversely, a point is outside a polygon if the ray intersects the polygon's edges an even number of times, or does not intersect at all.

Using this procedure, the predicted feasible region of the reduced model is constructed (Fig. 7) from the knowledge of the boundary points of the feasible region and using the point-in-polygon test for each randomly generated query point. The predicted region was found to cover almost 71% of the actual feasible region of the reduced model, obtained by grid search. Given the nonconvex nature of the feasible region, this is a very good estimate as compared to the ex-

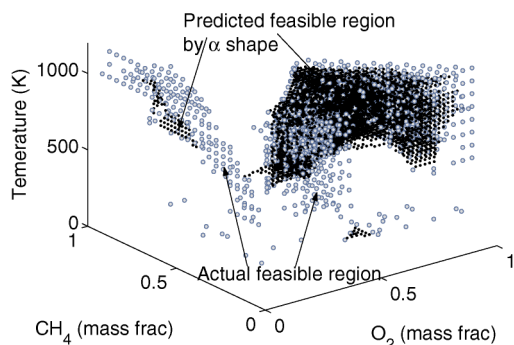


Fig. 7. Predicted feasible region of a reduced model.

isting approaches of feasibility analysis. However, it is possible to further improve the approximation by performing a more exhaustive sampling of the feasible space.

#### 4. Adaptive reduction

An efficient scheme having been determined for obtaining reduced kinetic models and evaluating the range of validity, the next step is the integration with the reacting flow simulation. The reactive flow model will typically span a broad range of species concentration and temperature. The detailed model retains information regarding the kinetic behavior of the system under all the different conditions of species concentration and temperature. However, when the detailed model is reduced, the reduced model loses such generality, since it retains information of system behavior under specific conditions given by its range of validity. If the same reduced model is used under all the conditions encountered in the reactive flow model irrespective of its validity, it will incorporate inaccuracy in the predictive capacity of the simulation. Hence the idea proposed in this work is to generate multiple reduced models addressing different conditions of the system. The flow simulation will use a particular reduced model only where it is feasible, meaning it retains its accuracy in prediction of the actual system behavior. Whenever the flow simulation encounters a condition for which the present selection fails, it will search for a different reduced model valid for such condition, and integrate it.

Thus, the main aim is to generate a library of reduced models, the feasible regions of which will together cover the entire range of conditions encountered in the reactive flow simulation. However, this requires a priori knowledge of the accessed region of the detailed reactive flow simulation which is not possible. An alternative method is to have an estimate of the accessed region by solving the detailed flow

simulation with a reduced mechanism or a simplified flow simulation with detailed kinetic mechanism. In the present work the pairwise mixed stirred reactor (PMSR) [10] model with detailed kinetic model is used for the estimation of the accessed region.

##### 4.1. Stochastic simulation of PMSR

At any time  $t$ , the PMSR consists of an even number  $N$  of particles, the  $i$ th particle having composition  $\phi^{(i)}(t)$ . The overall simulation of PMSR proceeds by first assigning initial conditions at  $t = 0$  to all the reactor particles, and then the simulation is advanced in discrete time steps until a statistically stationary state is attained. Between these discrete times, the composition evolves by a mixing fractional time step and a reaction fractional time step. In PMSR, the reactor particles are arranged in pairs such that particles 1 and 2, 3 and 4, ...,  $N - 1$  and  $N$  are partners. The mixing fractional step consists of pairs  $(p$  and  $q)$  evolving by a simple first-order linear model,

$$\begin{aligned} \frac{d\phi^{(p)}}{dt} &= -(\phi^{(p)} - \phi^{(q)})/\tau_{\text{mix}}, \\ \frac{d\phi^{(q)}}{dt} &= -(\phi^{(q)} - \phi^{(p)})/\tau_{\text{mix}}, \end{aligned} \quad (12)$$

where  $\tau_{\text{mix}}$  is the specified mixing timescale. The other physical processes present in the PMSR model are inflow and outflow to and from the reactor and reassignment of particle pairs, which ensures mixing between all particles in the reactor. With  $\tau_{\text{res}}$  being the specified residence time, outflow and inflow consist of selecting  $1/2N \Delta t / \tau_{\text{res}}$  pairs at random and replacing their compositions with inflow compositions, which are drawn from a specific distribution. With  $\tau_{\text{pair}}$  being the specified pairing timescale,  $1/2N \Delta t / \tau_{\text{pair}}$  pairs of particles (other than the inflowing particles) are randomly selected for pairing. Then these particles and the inflowing particles are randomly shuffled so that they have the probability of changing partners.

The parameter values used in the PMSR simulation are given in Table 2. The simulation consists of inflowing streams of  $\text{O}_2$ ,  $\text{N}_2$ , and  $\text{CH}_4$ , preheated to a temperature of 1200 K. The inflow rates of  $\text{O}_2$  and  $\text{CH}_4$  are 0.348:0.154, and the pressure is atmospheric throughout. Fig. 8 illustrates the accessed region for PMSR in temperature– $\text{CH}_4$ – $\text{O}_2$  space for this simulation. It is observed that a considerable portion of the temperature and species composition space is accessed by the PMSR simulation, and hence provides a satisfactory initial estimate of the composition space accessed in a more rigorous reactive flow model.

Table 2  
Parameters used in the PMSR simulation

Number of particles	$N$	500
Residence time	$\tau_{\text{res}}$	10 ms
Mixing timescale	$\tau_{\text{mix}}$	1 ms
Pairing timescale	$\tau_{\text{pair}}$	1 ms

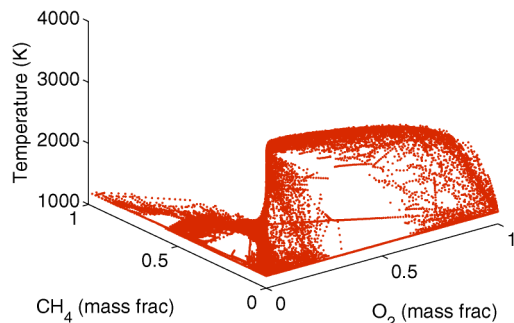


Fig. 8. Accessed region for a PMSR.

#### 4.2. Analysis of the accessed region

Having obtained an estimate of the accessed composition space, the next objective is to generate reduced reaction models which can cover the entire accessed space. This requires identification of nominal points at which reduction should be performed. This can be achieved by clustering the data of temperature and species concentration to identify patterns in the data set and obtain representative points for such patterns.

Data clustering is a branch of data mining problem. Given a large set of multidimensional data points, the data space is usually not uniformly occupied. *Data clustering* identifies the sparse and the crowded places, and hence discovers interesting data distributions and patterns in the underlying data. The problem of clustering can be defined as follows: given  $n$  data points in a  $d$ -dimensional metric space, partition the data points into  $k$  clusters such that the data points within a cluster are more similar to each other than data points in different clusters. Clustering techniques have been studied extensively in many different fields such as statistics, machine learning, and data mining, with numerous methods proposed and studied.

In recent years, a number of clustering algorithms have been proposed for large databases [28–30], which works well for convex or spherical clusters of uniform size, but are not suitable for nonspherical clusters having varied sizes.

As observed in Fig. 8, the data set in the present problem, which is the accessed region determined by the PMSR in the temperature–composition space, is large and nonconvex and is not uniform in shape,

hence eliminating the possibility of using the above algorithms. For clustering such arbitrary-shaped collections of points, a density-based algorithm called DBSCAN was proposed in Ester et al. [31], which works on two user-defined parameters: the radius Eps of the neighborhood of a point and the minimum number of points MinPts in the neighborhood. While DBSCAN can find clusters with arbitrary shapes, it has the problem of being extremely sensitive to the parameters and not being very robust. A recently proposed hierarchical based algorithm named CURE (clustering using representatives) [32] has the salient features of recognizing arbitrary-shaped clusters, having a linear storage requirement and a time complexity of  $O(n^2)$  for low-dimensional data, and is also stable. CURE adopts a middle ground between the centroid-based and all-point extremes. It starts by selecting a constant number  $c$  of well-scattered points, which are next shrunk toward the centroid of the cluster by a fraction  $\alpha$ . These points are used as representative of the cluster, and the clusters with the closest pair of representative points are merged at each step of the algorithm. The  $c$  representative points help in capturing the physical shape and the geometry of the cluster, and shrinking these points gets rid of surface abnormalities and mitigates the effect of outliers. The kind of clusters identified by CURE can be tuned by varying the value of  $\alpha$  between 0 and 1. It reduces to centroid-based algorithm for  $\alpha = 1$ , and to all points approach for  $\alpha = 0$ . It uses space that is linear in input size  $n$  and has a worst-case time complexity of  $O(n^2 \log n)$ . In the present work CURE has been used to cluster the datasets, and it was observed that considering a larger number of representative points indeed captured the shape of the cluster better than having a single point.

#### 4.3. Generation of library of reduced model

The clusters having been obtained, and the representative points for each cluster, one of the cluster centers is chosen at which mechanism reduction is performed following the procedure illustrated in Section 2, where first the detailed kinetic model is formulated for species reduction at the initial condition given by the cluster center, to arrive at an intermediate reduced model. This model is further reduced by the formulation of reaction reduction, to come up with the final reduced kinetic model at the particular initial condition. The next step is the determination of the range of validity of the reduced model within which it retains the desired accuracy. This requires an estimate of the feasible region, which can be obtained by sampling the temperature–composition space following the technique described in Section 3. To obtain a mathematical definition of this feasible space, an  $\alpha$

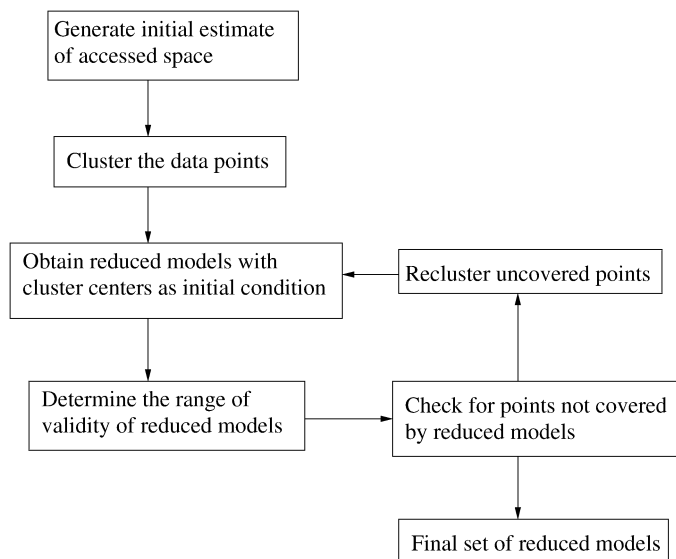


Fig. 9. Overall algorithm for adaptive reduction.

shape is constructed, which identifies the boundaries of the feasible space. The accessed data points are then checked to identify points which lie inside the generated feasible region using the point-in-polygon strategy. The feasible points are removed and the updated data set is reclustered to obtain another nominal point for reduction. This procedure is followed iteratively, as illustrated in Fig. 9, until enough reduced mechanisms are generated to cover the entire accessed region. The reclustering procedure is necessary since the feasible points for a particular reduced mechanism can cover an entirely different region than defined by the initial cluster for which the nominal point was the cluster center. Hence by the proposed iterative procedure the optimum number of reduced mechanisms covering the entire accessed space of the PMSR is obtained.

For the present simulation for methane combustion, a total of 12 reduced sets were generated, covering 78% of the region accessed by the PMSR model. All the reduced models were obtained by running GA with a population size of 10, evolved through 500 generations, with an allowable error of 0.01. The details of the size of all the reduced models are given in Table 3. It also compares the average CPU time required to integrate each of the reduced model. The CPU time required to integrate the detailed GRI-3.0 mechanism is 7.99 s, which is much higher than the reduced models.

All of these reduced models are obtained under different conditions of temperature and fuel and O<sub>2</sub> concentration. In order to ensure that the models indeed captured the physics of the system, the reduced models were tested for the known behavior of the sys-

Table 3

Reduced models used for adaptive simulation

Reduced mechanism	Size of mechanism		Single integration CPU (s)
	$N_{\text{species}}$	$N_{\text{reactions}}$	
1	6	5	0.015
2	9	19	0.037
3	17	25	0.605
4	18	28	0.01
5	22	50	0.188
6	25	51	0.265
7	22	54	0.023
8	27	74	0.026
9	26	84	0.696
10	27	104	0.048
11	28	117	0.096
12	29	150	0.18

tem. For example, nitrogen oxide formation is known to be absent at low temperatures and takes place only at higher temperatures. Similar behavior is observed in the reduced models, where the nitrogen oxide reactions were absent from the low-temperature reduced models and appear in the high-temperature mechanisms. Also, the high-temperature mechanisms included the endothermic dissociation reactions, which are absent from the low-temperature mechanisms, which is also a physical behavior. The reduced models obtained at high temperature are also consistent with the high-temperature methane oxidation mechanism discussed in Glassman [33].

Once sufficient number of reduced reaction models have been developed to cover the entire estimated accessed region, the next step is the incorporation of the reduced sets in the reactive flow models.

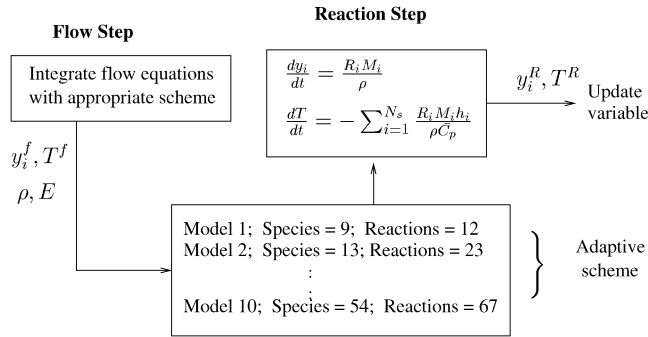


Fig. 10. Integration with flow simulation.

## 5. Integration with flow simulation

### 5.1. Modeling reactive flows

In the present work the stochastic reactor simulation of a pairwise mixed stirred reactor (PMSR) is used to test the performance of the adaptive reduction scheme. The PMSR scheme covers a broad range of conditions in the composition state space and it does not require an extensive modeling effort, hence offering a perfect testbed for judging the performance of the proposed scheme.

As mentioned before, the PMSR simulation is a time-marching scheme, where the incremental time step is split into the mixing time step and the reaction time step. For such a fractional time-stepping approach, the flow time-stepping will remain unaltered. This time step will result in a set of species concentrations and temperatures that are passed on to the reaction time step, at which the system will react under the conditions obtained from the flow time step. This reaction step requires the integration of a set of coupled stiff ODEs, which needs to be integrated over the reaction time step. When the detailed model is used for kinetic source term, all the  $N_s$  ODEs consisting of  $N_R$  reaction terms need to be integrated. The objective of the reduced model is to reduce the number of ODEs and their coupling by eliminating species and reactions participating in the source term. When a single reduced reaction model is used over the entire flow simulation, the same set of reduced ODEs needs to be integrated at the reaction step. In the adaptive chemistry scheme, however, there is a library of mechanisms from which the most appropriate one needs to be selected and integrated. Hence at every time it is likely that a different set of reduced ODEs are integrated. As discussed before, the accuracy of the reduced model depends solely on the initial species concentration and temperature at which it is used. Also, each reduced set is characterized by an  $\alpha$  shape defining the range of conditions over which it is accurate. Hence to select an appropriate reduced

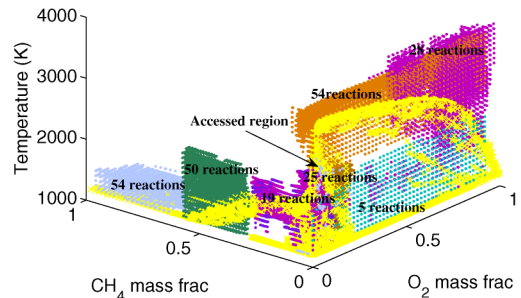


Fig. 11. Range of conditions addressed by different reduced models.

mechanism during the PMSR simulation, one needs to check the feasible region of all the mechanisms by performing the point-in-polygon test to determine one which is feasible at the local condition (Fig. 10). This check is a relatively inexpensive operation, on average taking 1 ms to check one point for a single reduced model. Hence, even for a fairly large library of reduced models, it is not expected to offset the computational savings achieved by the use of reduced models. The flow time step will involve the solution of all the species of the detailed mechanism, while the reaction time step will consider only those species present in the selected reduced model, and the concentration of all the other species will remain unaltered. This procedure was followed for PMSR simulation for methane combustion. The library of reduced sets presented in Table 3 is used along with their corresponding feasible region, which is the information of points forming the boundary of their range of validity. Depending on the local condition of the reactor, different reduced models were chosen by the flow simulation. Fig. 11 illustrates the different ranges of conditions addressed by different reduced model.

As is observed in the figure, most of the reduced models have overlaps in the feasible region. This means that more than one reduced model is valid under certain conditions. When such a situation arises, it is judicious to choose the smallest of all the valid

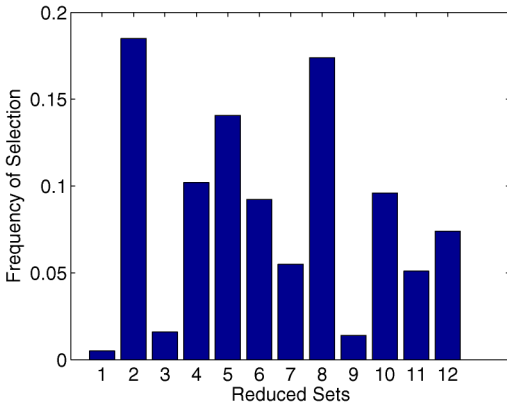


Fig. 12. Frequency of selection and integration of different reduced models.

models. With this aim, the library of the models are arranged according to increasing number of reactions. When the flow simulation accesses this library, it will come out of the library on identifying first valid model. This procedure was followed for the PMSR simulation of  $\text{CH}_4$  combustion, when the 12 reduced models were found to cover 78% of the conditions encountered by the flow simulation. For the remaining 22% of the conditions there was no valid reduced model in the library; hence the simulation integrated the detailed model for these conditions. The library can be further updated by obtaining valid reduced chemistry models for conditions not addressed by the present library.

For the PMSR simulation, at every time step all the reactor particles are under different conditions of species concentration and temperature, depending on which it selects an appropriate mechanism. Hence at every time step each of the reduced models was selected, but with different frequency. The reduced models chosen with higher frequencies can be consid-

ered to affect the reactor condition the most. Fig. 12 illustrates the average frequency at which different reduced models of the library were chosen by the simulation. The PMSR simulation was also performed using a single reduced set for the entire flow simulation and Figs. 13 and 14 illustrate the performance of adaptive reduction in the prediction of the species and temperature profiles as compared to using a single reduced model. The adaptive scheme could predict the temperature profile with an average error of 0.162% and a maximum deviation of 1.37%, whereas the single reduced model had an error of 1% and 6.1%, respectively. In the prediction of  $\text{CH}_4$  the adaptive scheme had an average error value of 0.05% and maximum deviation of 0.81%, and the single reduced model had one of 0.4% and 3.33%. The prediction of both the  $\text{O}_2$  and  $\text{O}$  profiles was more accurate for the adaptive scheme, having a maximum error of 1.07% and 1.9%, respectively, while the corresponding values for the single reduced model was 5% and 71%. The average size of the reduced model used for the adaptive scheme is approximately 54, while that of the single model was 59. This shows that by adapting the reduced model to the changing condition of the flow simulation, greater accuracy can be obtained with the same dimension of the reduced model.

The developed library of reduced model is further tested by applying it to PMSR simulations performed at conditions different from the one based on which the library was generated. This was done to check for the efficiency of the developed library for simulations under different conditions, and validate its consistency. Two such simulations were performed under different conditions of  $\text{CH}_4$  and  $\text{O}_2$  mass flow rates, given by (Case 1)  $\text{CH}_4:\text{O}_2:\text{N}_2 = 0.085:0.83:0.085$ , (Case 2)  $\text{CH}_4:\text{O}_2:\text{N}_2 = 0.245:0.538:0.217$ , both at atmospheric pressure and inlet temperature 1200 K. The developed library of reduced models was found to contain feasible mechanisms for an appreciable

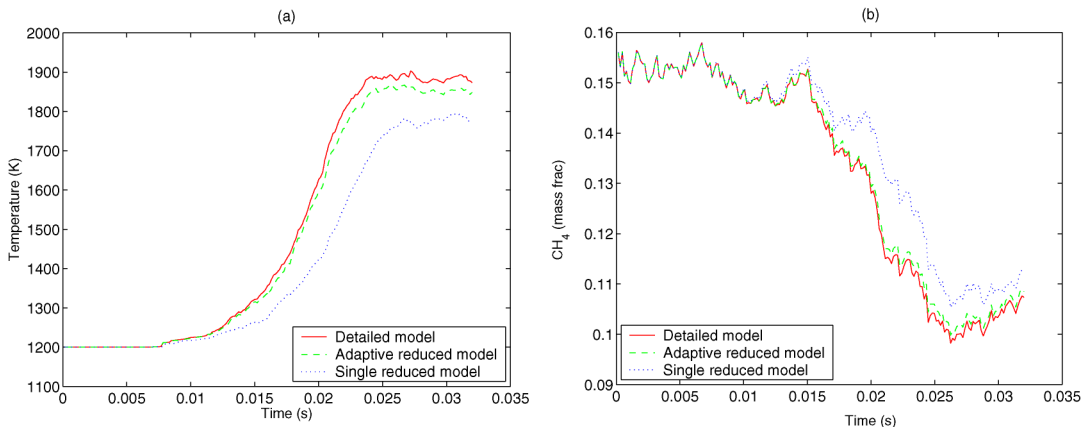


Fig. 13. Performance of adaptive reduction in the prediction of (a) temperature and (b) methane profile.

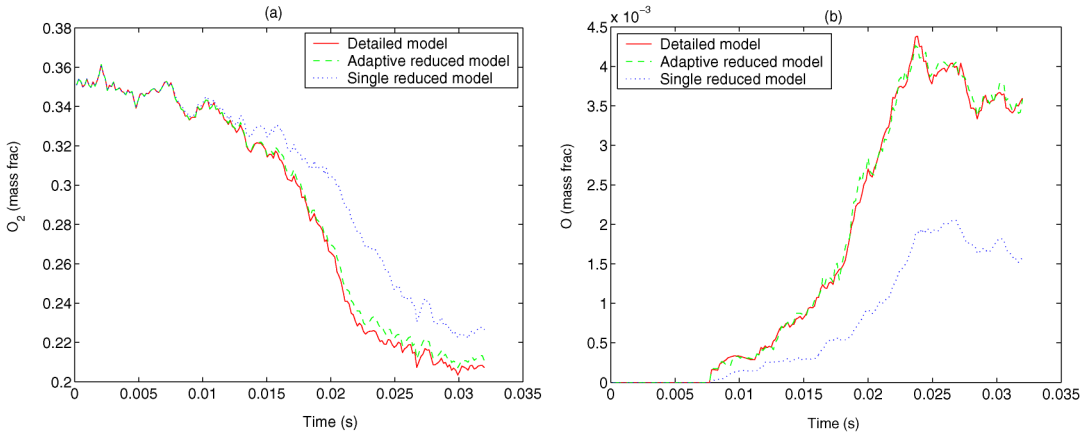


Fig. 14. Performance of adaptive reduction in the prediction of (a)  $O_2$  and (b)  $O$  profile.

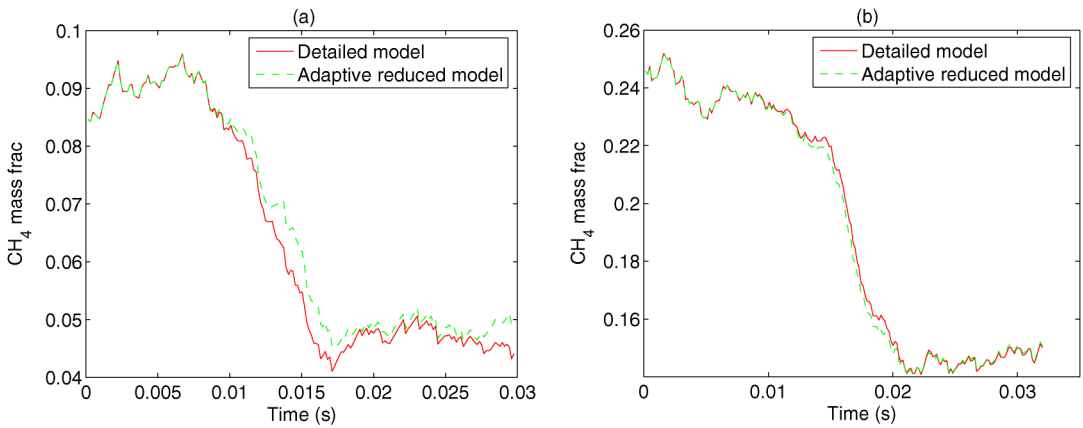


Fig. 15. Performance of adaptive reduction in the prediction of  $CH_4$  profile for (a) Case 1 and (b) Case 2.

fraction of both simulations, even though the reduced models were not generated for these particular test cases. This is an important part of the adaptive scheme, since it indicates that the library is general and once it is generated, it can be used in simulations under different conditions and configurations. The generality of the developed library is mainly attributed to the feasibility analysis step, which captures the conditions of temperature and  $CH_4$  and  $O_2$  concentrations at which the reduced model is valid. The accuracy of prediction of the temperature and  $CH_4$  and  $O_2$  profiles for these two test cases is given in Table 4. Fig. 15 compares the prediction of the  $CH_4$  profiles for the above two test cases.

## 6. Discussion

In the proposed work an adaptive reduction scheme is developed to replace the detailed complex kinetic network with a set of simple reduced networks, which can predict the behavior of the detailed model with

Table 4

Error measure by using the library of reduced model for the test cases

% error	Case 1	Case 2
Temperature	2.37	0.7
$CH_4$	3.12	0.38
$O_2$	0.98	0.14

high accuracy within a limited range of conditions. The procedure involves generating an initial estimate of the range of conditions encountered in a practical reactive flow simulation. This is followed by identification of nominal points at which mechanism reduction needs to be performed. An efficient two-step mechanism reduction scheme based on mathematical programming approach has been discussed in details. Having obtained a reduced model at a nominal point, the next step is the determination of the range of conditions over which this mechanism retains its accuracy. A new feasibility analysis procedure based on surface reconstruction methodology is presented to

describe the feasible region of each reduced model. For the present work, the local condition of temperature and CH<sub>4</sub> and O<sub>2</sub> concentration are used as the basis for selection of a feasible reduced model. While these three parameters were found to be adequate in defining the state of CH<sub>4</sub> combustion, they are likely to change depending on the description of the fuel.

The integration of the adaptive scheme in a pairwise mixed stirred reactor is also presented. Since the PMSR spans a large area in the composition–temperature space, it provides a stringent test for any reduced chemistry scheme. The excellent performance of the proposed scheme in the PMSR simulation does illustrate the potential of the approach and indicates the suitability of this approach in a more rigorous flow simulation.

The adaptive reduced models are generated to cover the range of conditions accessed by a particular PMSR simulation. However, when the feasibility of a reduced model is determined, a much broader range of composition and temperature is considered, which is not limited to the PMSR simulation. Hence the feasibility of the generated reduced models is much larger than the accessed region of the PMSR simulation. Even then, while incorporating the adaptive scheme in a more rigorous flow simulation one may encounter conditions for which no appropriate reduced model is available. For such cases one option is to use the detailed model under those conditions, and the other option is to build a reduced model for those initial conditions, describe its validity range, and update the library of reduced models.

## Acknowledgments

The authors gratefully acknowledge financial support from the donors of the Petroleum Research Fund, administered by the ACS and the Office of Naval Research under Contract N00014-03-1-0207 and by the National Science Foundation (CTS 0224745). The genetic algorithm code used in this paper was originally developed by David L. Carroll.

## References

- [1] A.S. Tomlin, T. Turanyi, M.J. Pilling, in: M.J. Pilling (Ed.), *Low-Temperature Combustion and Auto Ignition*, in: *Comprehensive Chemical Kinetics*, vol. 35, 1997.
- [2] N. Peters, *Prog. Astronaut. Aeronaut.* 113 (1988) 67.
- [3] T. Turanyi, K. Hughes, M. Pilling, A. Tomlin, *KINALC: Program for the Analysis of Reaction Mechanisms, Combustion Simulations at the University of Leeds*, 1996.
- [4] J.-Y. Chen, *Workshop on Numerical Aspects of Reduction in Chemical Kinetics*, Academic Press, New York, 1974.
- [5] C. Sung, C. Law, J.-Y. Chen, *Combust. Sci. Technol.* 156 (2000) 201.
- [6] C. Sung, C. Law, J.-Y. Chen, *Combust. Flame* 125 (2001) 906.
- [7] M. Frenklach, in: W.C. Gardiner (Ed.), *Modeling, Combustion Chemistry*, Springer-Verlag, New York, 1984.
- [8] S.H. Lam, D.A. Goussis, *Int. J. Chem. Kinet.* 26 (1994) 461.
- [9] U. Mass, S.B. Pope, *Combust. Flame* 88 (1992) 239.
- [10] S.B. Pope, *Combust. Theory Model.* 1 (1997) 41.
- [11] I.P. Androulakis, *AIChE J.* 46 (2000) 361.
- [12] L. Petzold, W. Zu, in: *AIChE Meeting*, Los Angeles, 1997.
- [13] I. Banerjee, M. Ierapetritou, *Chem. Eng. Sci.* 58 (2003) 4537.
- [14] D. Schwer, P. Lu, W. Green, *Combust. Flame* 133 (2003) 451.
- [15] G. Smith, D. Golden, M. Frenklach, N. Moriarty, B. Eiteneer, M. Goldenberg, C. Bowman, R. Hanson, S. Song, W. Gardiner, V. Lissianski, Z. Qin, [http://www.me.berkeley.edu/gri\\_mech/](http://www.me.berkeley.edu/gri_mech/).
- [16] K. Edwards, T. Edgar, V.I. Manousiouthakis, *Comput. Chem. Eng.* 22 (1998) 239.
- [17] D.E. Goldberg, *Genetic Algorithms in Search, Optimization and Machine Learning*, Addison–Wesley, New York, 1989.
- [18] Z. Michalewicz, M. Schoenauer, *Evol. Comput.* 4 (1996) 1.
- [19] A.C. Hindmarsh, in: R.S. Stepleman, et al. (Eds.), *Scientific Computing*, North Holland, Amsterdam, 1983.
- [20] R. Kee, F. Rupley, E. Meeks, J.A. Miller, *CHEMKIN-III: A Fortran Chemical Kinetics Package for the Analysis of Gas-Phase Chemical and Plasma Kinetics*, Sandia Report SAND96-8216, 1996.
- [21] B. Bhattacharjee, D. Schwer, P. Barton, W.H. Green, *Combust. Flame* 135 (2003) 191.
- [22] R. Swaney, I. Grossmann, *AIChE J.* 31 (1985) 621.
- [23] I. Banerjee, M. Ierapetritou, *Ind. Eng. Chem. Res.* 44 (2005) 3638.
- [24] H. Edelsbrunner, D. Kirkpatrick, R. Seidel, *IEEE Trans. Inform. Theory* IT-29 (1983) 551.
- [25] H. Edelsbrunner, E.P. Mucke, *ACM Trans. Graph.* 13 (1) (1994) 43–72.
- [26] D. Mandal, C. Murthy, *Pattern Recogn.* 30 (1997) 1759.
- [27] E. Haines, in: P. Heckbert (Ed.), *Graphic Gems*, Academic Press, 1994, p. 24.
- [28] T. Raymond, J. Han, in: *Proc. of the VLDB Conference*, Santiago, Chile, 1994.
- [29] M. Ester, H. Kriegel, X. Xu, in: *Int. Conf. on Knowledge Discovery in Databases and Data Mining*, Montreal, Canada, 1993.
- [30] T. Zhang, R. Ramkrishnan, M. Livny, in: *Proc. of the ACM SIGMOD Conf. on Management of Data*, Montreal, Canada, 1996.
- [31] M. Ester, H. Kriegel, J. Sander, X. Xu, in: *Int. Conf. on Knowledge Discovery in Databases and Data Mining*, Montreal, Canada, 1996.
- [32] S. Guha, R. Rastogi, K. Shim, *Proc. ACM SIGMOD* (1998) 73.
- [33] I. Glassman, *Combustion*, Academic Press, 1996.